Materials Today Communications 8 (2016) 53–63

Contents lists available at ScienceDirect

Materials Today Communications

journal homepage: www.elsevier.com/locate/mtcomm

"Polymer-polymer composites for the design of strong and tough degradable biomaterials"

Xi Zhang [a], Mike A. Geven [b], Dirk W. Grijpma [b,c], Julien E. Gautrot [a,d,*], Ton Peijs [a,e,*]

[a] School of Engineering and Materials Science, Queen Mary University of London, Mile End Road, London E1 4NS, UK
[b] MIRA Institute for Biomedical Technology and Technical Medicine, Department of Biomaterials Science and Technology, University of Twente, 7500 AE Enschede, The Netherlands
[c] University Medical Center Groningen, W.J. Kolff Institute, Department of Biomedical Engineering, University of Groningen, 7600 AD Groningen, The Netherlands
[d] Institute of Bioengineering, Queen Mary University of London, Mile End Road, London E1 4NS, UK
[e] Nanoforce Technology Ltd., Joseph Priestley Building, Queen Mary University of London, Mile End Road, London E1 4NS, UK

ARTICLE INFO

Article history:
Received 26 May 2016
Accepted 30 May 2016
Available online 2 June 2016

Keywords:
Short electrospun fibres
Nanofibre-reinforced composites
Mechanical properties

ABSTRACT

Polylactide (PLA) fibre reinforced poly(trimethylene carbonate) (PTMC) composites were prepared by incorporating electrospun fibres in tri-functional methacrylate-terminated PTMC macromer solutions and cured by UV irradiation. Short electrospun fibres with average length of 50–700 μm were prepared by solvent assisted mechanical stirring and different amounts of short fibres were loaded into PTMC composites. The reinforcement effect of short PLA fibres at different concentrations and continuous fibre were assessed by tensile tests and micromechanical models. With the incorporation of continuous electrospun PLA fibres, the Young's modulus of PTMC was increased from 2.7 to 310 MPa; while tensile strength and toughness were also improved significantly. The addition of small amounts (5 wt%) of short PLA fibres increased the Young's modulus and tensile strength three-fold without compromising the ductility of PTMC. The potential to tailor the mechanical performance and dimensional stability of these nontoxic and degradable PTMC/fibre composites makes them interesting candidates for tissue engineering applications.

1. Introduction

Poly(trimethylene carbonate) (PTMC) is a biodegradable elastomeric material with potential application in tissue engineering. The polymerization of PTMC has been reported since 1932 [1] and is currently most often carried out via the ring-opening polymerisation of 1,3-trimethylene carbonate [2]. Unlike degradable polyesters, due to its poor mechanical properties it has not been extensively used in practical applications. However, its low glass transition temperature and rubber-like properties have made it a good candidate as a soft component in the design of composites or copolymers. PTMC has been incorporated in blends or in the structure of block copolymers with rigid biodegradable polymers such as PLA to introduce toughness whilst preserving degradability [3–5]. In addition, Pêgo et al. showed that at very high molecular weight, PTMC can exhibit much improved mechanical properties and dimensional stability [6]. In addition to increasing molecular weight, crosslinking was found to be another way to achieve stable PTMC morphologies. This was achieved, for example, via gamma irradiation [6]. However, high energy irradiation can result in polymer chain scission, which can affect the mechanical performance of the material. To avoid adverse chain scission effects, crosslinkers have been incorporated into the structure of PTMC polymers to produce PTMC networks with improved mechanical properties [7]. Bat et al. incorporated methacrylate groups into PTMC macromers (branched and linear) and crosslinked them in a mixture with PTMC homopolymer upon UV exposure. The resulting material showed excellent dimensional stability and a reduced surface erosion rate compared to linear PTMC [8]. The photo crosslinking technique was considered to be highly efficient and could be completed at room temperature. It was subsequently reported that direct crosslinking of methacrylate-ended PTMC macromers without linear PTMC could also produce strong and tough materials [9]. On the other hand, incorporating nanoparticles such as tricalcium phosphate into PTMC produced composite materials with

* Corresponding authors at: School of Engineering and Materials Science, Queen Mary University of London, Mile End Road, London E1 4NS, UK
E-mail addresses: j.gautrot@qmul.ac.uk (J.E. Gautrot), t.peijs@qmul.ac.uk (T. Peijs).

http://dx.doi.org/10.1016/j.mtcomm.2016.05.001
2352-4928/

improved mechanical properties, displaying improved bone formation [10]. Nevertheless, one potential issue with PTMC/nanoparticle composites is the weak interaction between filler and matrix as weak bonding can potentially trigger failure especially after prolonged usage [11]. In addition, reinforcement can only be achieved at relatively high nanoparticle-loading (for β-tricalcium phosphate, 30 vol% loading was reported to increase the flexural modulus of PTMC from 6 to 17 MPa [10]) and the use of fillers with higher shape aspect ratios, such as fibres, would be required to reduce the loading requirements.

Electrospinning is a widely used technique for generating micro/nano fibres [12,13]. The ease of fabrication, large surface area and aspect ratio of electrospun fibres are believed to make them very suitable as reinforcements for soft polymeric materials. However, relatively few reports have presented the use of electrospun fibres to reinforce composites [11,14–18]. Bergshoef and Vancso incorporated nylon-4,6 electrospun fibres into epoxy resin and produced electrospun fibre reinforced transparent composite [14]. Stachewicz et al. manufactured electrospun nylon 6 fibres-PVA composite with optimized mechanical properties [16]. Yao et al. fabricated high performance unidirectional co-polyimide nanofibre reinforced composites by impregnating fibre mats with styrene-butadiene-styrene block copolymer solutions [17]. Zuo et al. loaded biodegradable electrospun fibres into calcium phosphate [18], with the addition of electrospun polymeric fibres increasing the material's fracture resistance, toughness, porosity and resorption rate. In spite of their interesting properties, the application of electrospun fibres as reinforcement in composites has often been limited because of their relatively poor mechanical properties compared to traditional high performance fibres such as glass or carbon, which is mainly ascribed to the low orientation and chain extension of polymer chains in most electrospun fibres [13]. The limitation of producing high performance electrospun fibre composite is also due to the difficulties of producing highly continuous and oriented electrospun fibres on a large scale [19]. Besides their relatively poor mechanical performance, which is typically limited to 2–4 times the Young's modulus of bulk polymer [13], electrospun fibre entanglement is another obstacle in composite fabrication when products of complex geometry or structure have to be manufactured. Electrospun fibre mats can suffer from poor homogeneity and poorly compatible with polymer matrices. Moreover, the continuous and entangled fibre mats limit their use in traditional polymer processing techniques like injection moulding, extrusion, 3D printing etc.

Jiang et al. reported the incorporation of short electrospun polyimide (PI) fibres into PI matrix and achieved as good self-reinforcement as when using continuous PI fibres [20]. Unlike conventional short fibres such as glass or carbon fibres [21,22], short electrospun fibres as reinforcements in polymer composites have received little attention. The use of such short fibres could greatly simplify the procedures associated with fibre integration in composites. In addition, electrospun polymeric fibre properties can be easily modified by changing the polymeric material, coating the fibres or adding functional groups, conferring new properties to the composite material [23]. Most importantly, the use of short fibres enables the creation of composites that have complex shapes and are moulded by traditional flow moulding processes such as extrusion, injection or compression moulding, vastly increasing their potential applications. However, self-reinforced PI/PI short fibre composites exhibited rather limited property improvements. More significantly reinforcements could be realised by using either stronger and stiffer fibres or softer matrices.

Polylactic acid (PLA) is a widely studied biodegradable polymer used as food packaging material and for the design of implants [24]. It can be derived from building blocks synthesised using renewable resources and is fully degradable. Moreover, it is much stiffer and stronger than PTMC. The modulus of PLA can be as high as 4 GPa [25], whilst the modulus of drawn PLA fibres and electrospun fibres can reach values as high as 8 GPa [26,27]. Depending on molecular weight, the Young's modulus of non-crosslinked/crosslinked PTMC for biomedical applications is usually below 10 MPa [9,10]. Thus, the incorporation of PLA electrospun fibres can be of interest for the improvement of mechanical properties as well as dimensional stability of PTMC. Meanwhile, the highly porous electrospun fibre network will also ensure that the volume fraction of PLA fibres is minimised when integrated into composite matrix. By minimising the amount of PLA, the risk of its acidic degradation products accumulation is also reduced, which could otherwise potentially induce tissue inflammatory responses [28]. Moreover, as PTMC is used in 3D printing for tissue engineering [29], the combination of PTMC with short electrospun PLA fibres can potentially enhance the range of applications targeted by this process. In this respect, the development of short PLA fibres is particularly important to enable 3D processing technologies such as stereolithography and 3D plotting to generate polymer–polymer composites with precise, tailored and complex 3D shapes.

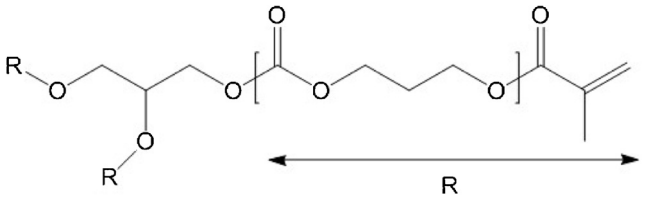

Fig. 1. Chemical structure of three-armed PTMC macromer with methacrylate end groups.

In this paper, we report the formation and characterisation of both long and short PLA electrospun nanofibre-reinforced PTMC composites. A reliable and scalable methodology to generate short PLA fibres from electrospun mats was developed. As a reference long fibre composites based on electrospun PLA fibre mats were impregnated with tri-functional methacrylate-terminated PTMC macromers, which was then crosslinked under UV to form PTMC/electrospun PLA nanofibre composites. The morphology and mechanical properties of neat PTMC and their long- and short fibre composites were characterized and discussed in relation to fibre length and loading. This work demonstrated the development of PTMC/nanofibre composites to be used as non-toxic, biocompatible, fully degradable and easily processable materials showing promising features for a variety of tissue engineering applications.

2. Experimental

2.1. Materials

The three-armed PTMC macromer, methacrylate terminated, with a molecular weight of 10,000 g/mol was prepared as previously described [30]. The chemical structure of the PTMC macromer is shown in Fig. 1. Poly(lactic acid) (PLA) 2002D was obtained from Natureworks (Mw 200,000 g/mol). Chloroform and dimethylformamide (DMF) were purchased from Fisher Scientific. Propylene carbonate and ethanol were purchased from Sigma Aldrich. Irgacure TPO-L and Orasol Orange 247 were obtained from BASF. All polymers and reagents were used as received.

2.2. Electrospinning of PLA fibres

PLA 2002D was dissolved in chloroform/DMF mixture with solvent ratio of 3/1. The PLA concentration was prepared at 9 wt% and was stirred until forming a homogeneous solution. The electrospinning was carried out using a home built electrospinning setup. A

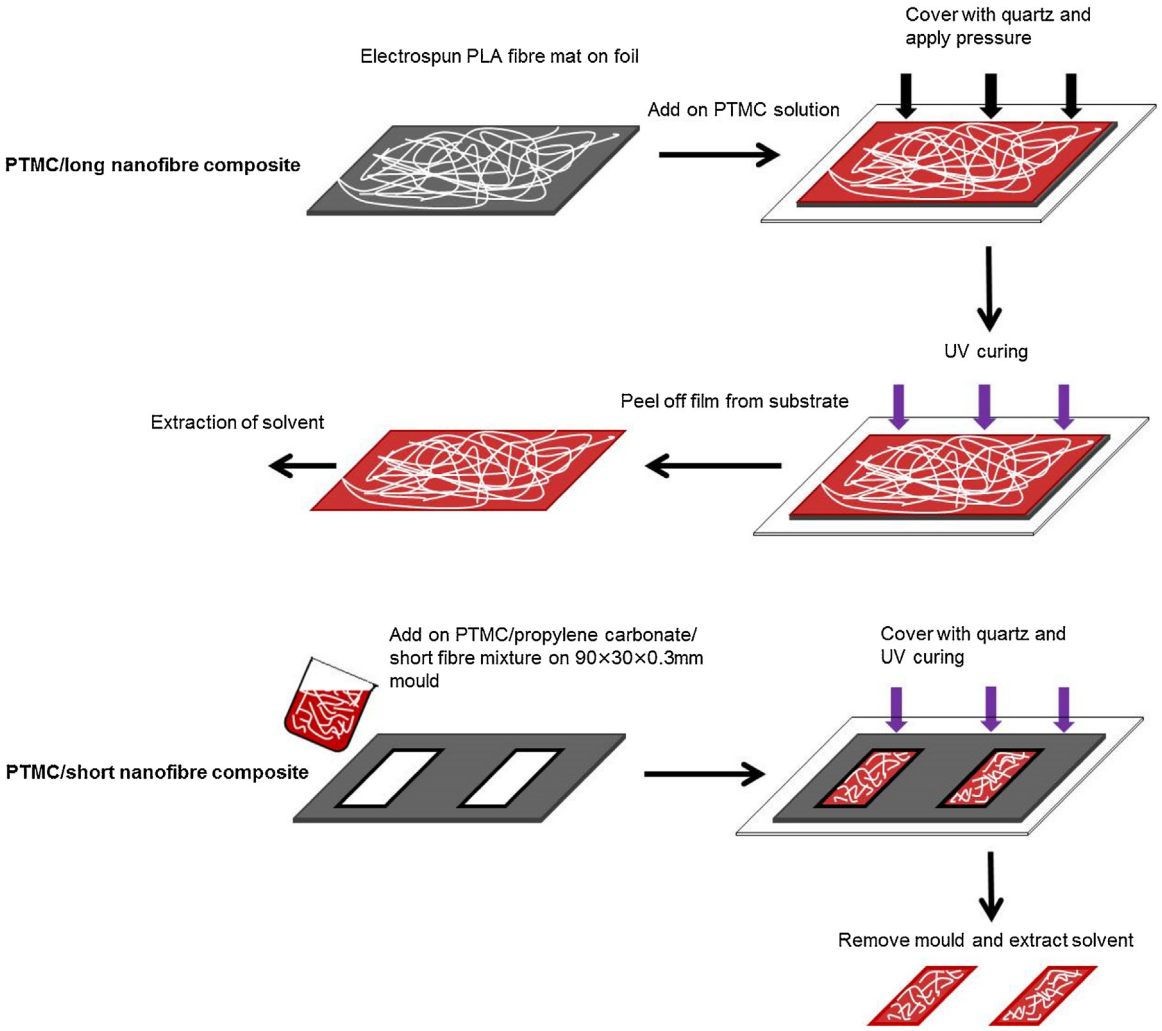

Fig. 2. Schematic representation of the fabrication process of long- and short PTMC/electrospun PLA nanofibre composite films.

syringe pump (Kent Genie) was used to continuously supply the PLA solution to the spinning tip at a feeding rate of 1.0 mL/h. A voltage of 18 kV (Glassman EQ) was applied to the spinning tip to charge and generate electrostatic forces, which overcomes the solution's surface tension and ejects a fluid jet. The fluid jet solidified during flight and was collected on aluminium foil. The achieved electrospun PLA fibre mats were left in a vacuum desiccator for 48 hrs to remove residual solvents prior to any further processing.

2.3. Fabrication of short electrospun fibres

Two different methods were tested for cutting continuous electrospun fibre mats into short fibres: ultrasonication and mechanical stirring. Both methods were carried out in a series of toluene/petroleum ether (T/P) mixtures as dispersant media. The sonicator (Sonics VCX500) was equipped with a 13 mm probe and had a frequency of 750 kHz. Electrospun fibre mats were placed in the media and sonicated at amplitude of 40% with 2 sec on and 2 sec off mode. The sonication lasted for 2 min. For the mechanical stirring method, fibre mats were simply placed in the media and stirred at 1500 rpm using a magnetic stirrer (IKA RET basic) for 24 hrs. For both techniques, the resultant fibres were collected first by sedimentation and carefully decanting most of the supernatant. Then the mixture was left to evaporate the media solvent in a fume hood overnight. Finally, the fibres were placed in vacuum desiccator for 48 hrs to remove residual solvent. During the experiment, one drop of each fibre dispersions was transferred onto glass slide with a pipette immediately after cutting. The glass slide was then left in fume hood to evaporate the solvent and used for SEM characterization.

2.4. Fabrication of PTMC/electrospun PLA fibre composites

PTMC resin was prepared by dissolving PTMC macromer in propylene carbonate, which is a non-volatile, stable solvent, fully compatible with PLA (does not dissolve or swell this material significantly). Three different PTMC concentrations were prepared, 20 wt%, 30 wt% and 40 wt%. PTMC was added to propylene carbonate and stirred until fully dissolved. Irgacure TPO-L and Orasol Orange 247 (used to control light intensity) were added into the PTMC/propylene carbonate solution at 5 wt% and 0.15 wt% (with respect to PTMC), respectively. This mixture was continuously stirred to form a homogeneous solution and was carefully transferred into a $90 \times 30 \times 0.3$ mm mould. A quartz plate was used to cover the mould to result in a flat and smooth top surface. The resin was exposed to UV (Omnicure 1500, 15 mW/cm^2) for 90 sec to achieve crosslinking and a high modulus. The cured films were then peeled from the substrate and incubated in propylene carbonate/ethanol media to extract propylene carbonate. The extraction solution was refreshed daily, starting with a ratio of propylene carbonate/ethanol of 50/50 and decreasing the propylene carbonate concentration by 10% steps every day until it was fully removed

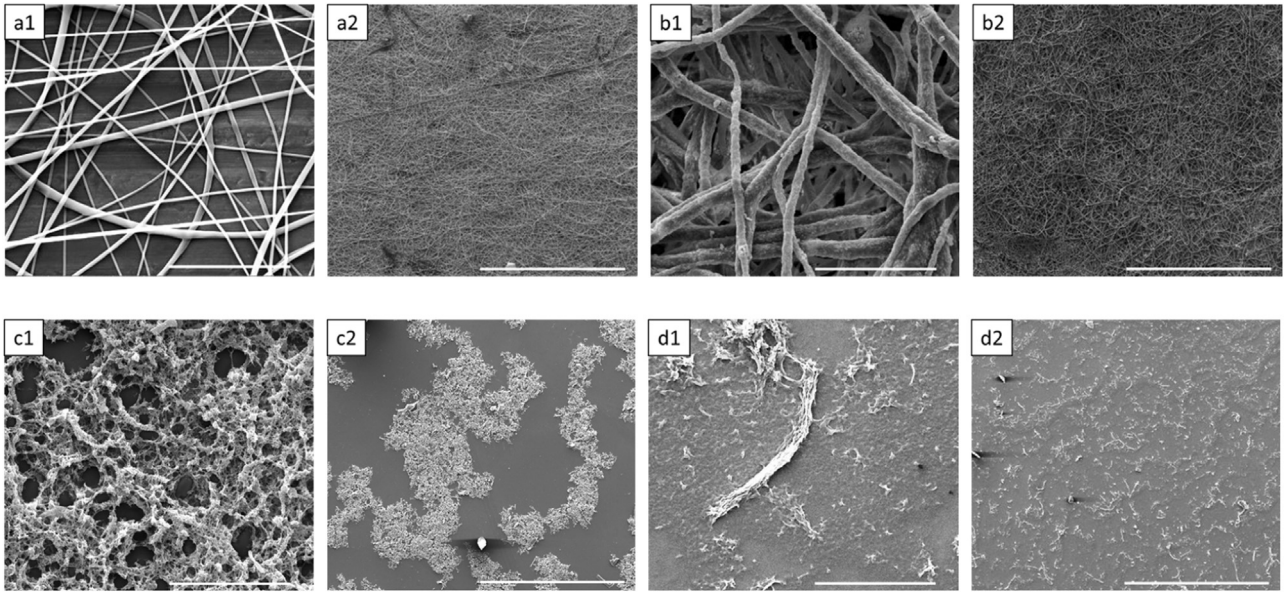

Fig. 3. SEM images of PLA electrospun nanofibres and cut fibres produced by ultrasonication: a1-a2, as-spun PLA fibres; b1-b2, sonication of PLA fibres in T/P=3/7; c1-c2, sonication of PLA fibres in T/P=6/4; d1-d2, sonication of PLA fibres in T/P=8/2. (scale bars: a1, b1, c1, d1, 20 μm; a2, b2, c2, d2, 400 μm).

from the mixture. The extracted composite film was then left in a fume hood to dry and weighed after drying.

The process of making PTMC/nanofibre composites is shown schematically in Fig. 2. Pre-weighed electrospun (random) fibre mats with a thickness of 100 μm were cut into 80 mm × 20 mm strips and placed on a flat and smooth substrate. 40 wt% PTMC/propylene carbonate solution was then used to impregnate the fibre mat while a quartz plate was placed on top. Gentle pressure was applied on the quartz plate to help the impregnation of the fibres as well as create a smooth surface. Moreover, excessive solution could be removed from the fibre mats to avoid resin-rich areas that could potentially form on the top surface. The impregnated fibre mats were left under pressure overnight to further improve impregnation. Next, the samples were cured by UV and extracted in the same way as described above. PTMC/short nanofibre composites were prepared by UV curing PTMC-short nanofibre mixtures (short nanofibres dispersed into PTMC/propylene carbonate solutions). Different amounts of short electrospun nanofibres (5 wt% and 30 wt% with respect to PTMC) were mechanically blended with PTMC/propylene carbonate solution (PTMC/propylene carbonate solutions were at a concentration of 40 wt%). The mixture was cast into a 90 × 30 × 0.3 mm mould and crosslinked under UV. The composites were then extracted in the same way as the long fibre composites.

2.5. Characterization

Scanning electron microscopy (SEM) (FEI Inspect F) was used to characterize both long and short electrospun PLA fibres. All SEM samples were coated with a thin gold layer before imaging. The imaging was performed at 10 mm distance and a voltage of 10 kV. Software Image J was used to analyse the average fibre diameter and length. To observe the interaction between fibres and matrix, samples were immersed and cold fractured in liquid nitrogen. The fracture surface was then coated with a thin gold layer and characterized using SEM.

Rheology was carried out with a rheometer (TA instruments DHR-3) to characterize rheological properties of the PTMC/propylene carbonate solution during UV exposure. The PTMC solution was placed between parallel plates of 20 mm diameter and a gap of 0.5 mm. The test was performed at a frequency of 1 Hz, a strain of 0.1% and a UV intensity of 15 mW/cm^2. Tensile tests were carried out using an Instron 5967 equipped with a 1 kN load cell at room temperature. All samples were cut into dumbbell shapes with size of 65 mm × 13 mm and thin centre part of 30 mm × 3 mm. Strain was taken from the displacement of the grip. The test was performed at a strain rate of 50 mm/min. Young's moduli were calculated from the slope of the stress-strain curve at low strain (2%). For each sample, three specimens were tested. In addition to tensile tests, dynamic mechanical analysis (DMA) (TA instruments Q800) was used to investigate the storage modulus of PTMC/fibre composites at different temperatures ranging from −50° C to 170° C. DMA was carried out at a heating rate of 3° C/min with a frequency of 1 Hz and a strain of 0.1%. Thermal properties were tested by differential scanning calorimeter (DSC, PerkinElmer DSC 4000). PLA electrospun fibres and PTMC/fibre composites were heated from 25° C to 180° C at a rate of 10° C/min. Neat PTMC was heated from −50° C to 180° C at a rate of 10° C/min. T_g is determined by the mid-point temperature of the materials' glass transition. The crystallinity of PLA fibres is calculated by,

$$X_c = \frac{\Delta H_m}{\Delta H_{ref}} \times \frac{1}{w} \times 100\%$$

where X_c is the crystallinity, ΔH_m is the experimental heat of fusion at melting point determined by DSC, ΔH_{ref} is the theoretical heat of fusion of fully crystalline PLA (93 J/g) [31] and w is the weight fraction of PLA in composites.

3. Results and discussion

3.1. Electrospinning of PLA and short nanofibre fabrication

In this study, two different routes were explored for the cutting of PLA electrospun nanofibres. SEM images of long and short electrospun PLA fibres are shown in Fig. 3 and 4. The electrospun fibres ranged in diameter from 300 nm to 1300 nm with an average diameter of 625 ± 278 nm. Fibres are continuous and smooth with no obvious defects (such as beads) observed (see Fig. 3 a1 and a2). A number of methods have been reported for the cutting of electrospun fibres, including ultrasonication [32,33], UV

cutting [34], cryogenic-cutting [20,35], direct spinning by tuning concentration and voltage [36], spinning with nanoparticles [37] or the use of a specific electrospinning setup [38]. Cryo-cutting is an up-scalable method of fibre cutting however we found PLA fibres remained relatively ductile even at low temperature, making the cutting difficult. Ultrasonication is easy to operate, with relatively standard equipment. The mechanism of this cutting method involves bubble cavitation and implosion, releasing energy that can result in the rupture of fibres. The method proved successful for the cutting of carbon nanotubes [39], however, its effectiveness is significantly reduced when using ductile polymer fibres. Hence, fibre pre-treatment such as irradiation have been used to generate weak points before ultrasonication in order to promote cutting [33]. In our work, we used a media composed of toluene and petroleum ether to facilitate the fragmentation of electrospun fibres. As PLA is hydrophobic, water was considered not suitable for ultrasonic cutting because of the poor interaction between water and fibres. Since fibre–fibre bonding is energetically favoured over fibre-water interactions, less water can infiltrate into the electrospun network, leading to less bubble cavitation and implosions [32]. Surface modification of the PLA fibres could improve its hydrophilicity but may affect its mechanical properties. The combination of toluene and petroleum ether is hydrophobic and readily wets the PLA fibre mat. Moreover, PLA is neither dissolving nor degrading in these two solvents at room temperature, thus the nature of fibres will not be affected. Water was also avoided to prevent hydrolytic degradation of PLA and to ensure that hydrophilic drugs that may be loaded in PLA fibres would not diffuse out prior to their incorporation in the PTMC matrix. Fig. 3b–d presents SEM images of PLA fibres processed by sonication in toluene/petroleum ether (T/P). They show cutting of the PLA fibres is promoted when the toluene concentration increases. This could be explained by the partial swelling of PLA in toluene. At a low volume fraction of toluene (T/P=3/7), the surface of fibres becomes rougher and pitted but no fracture was observed. Increasing the toluene concentration raised the swelling of PLA in the media. Fibres started adhering to each other and the network began to break down (T/P=6/4), finally leading to the collapse of the fibres. Fibre morphology was severely damaged at 80% toluene (T/P=8/2). Short fibres are generated at this T/P ratio however fibres' mechanical properties are significantly influenced due to the morphology damage. Thus these fibres were considered not suitable for PTMC reinforcement.

To maintain the morphology of short fibres, mechanical stirring was used which generates less local heating than ultrasonication. The impact of solvent composition (10–100% toluene in petroleum ether) used to suspend nanofibres during mechanical stirring was studied. It was found that at toluene concentrations approaching 80%, the electrospun fibre mats started to disentangle as well as fragment (see Fig. 4a). In addition, fibres maintained their morphology rather than collapse and there was little sign of solvent-induced damage, despite the high toluene concentration. Stirring in 100% toluene led to swelling and partial dissolution of the PLA fibres and their deformation. Stirring in 80% toluene media produced fibre lengths ranging from 50 μm to 700 μm. The characterisation of the length distribution obtained is summarized in Fig. 5. The average length of the PLA fibres made by this method is 220 ± 112 μm with the majority of the cut fibres between 100 and 200 μm in length. Compared with ultrasonication, mechanical stirring could cut these ductile electrospun PLA fibres without damaging their morphology or requiring any pretreatments. Compared to other techniques such as UV or cryogenic milling, mechanical stirring is simple, accessible and scalable. Moreover, this technique did not lead to the degradation of PLA molecules as is the case in UV or laser processing, preserving the properties of fibres.

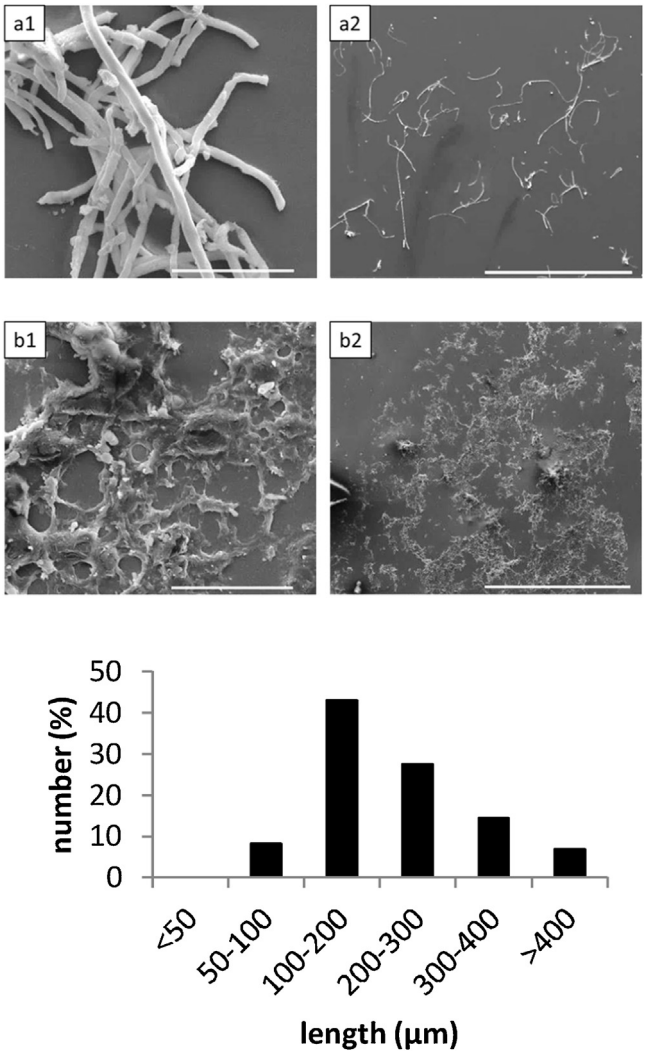

Fig. 4. Characterisation of fibres cut by mechanical stirring. (upper) SEM image of cut PLA fibres produced by mechanical stirring: a1-2, stirring of PLA fibres in T/P 8/2; b1-2, stirring of PLA fibres in T/P 10/0; scale bars: a1, b1, 20 μm, a2, b2, 400 μm. (below) length distribution of cut fibres produced by mechanical stirring in T/P=8/2 with average length at 220 ± 112 μm.

3.2. Fabrication of PTMC and PTMC/nanofibre composites

The PTMC and PTMC/PLA fibre composites were prepared by the crosslinking of the methacrylate end groups under UV irradiation. Photo-rheology was performed to study the rheological behaviour of the PTMC macromer in propylene carbonate resin during UV curing before the preparation of the PTMC composites. Three different concentrations of PTMC in propylene carbonate were tested (20, 30 and 40 wt%). To achieve optimal viscosity of the solutions for impregnation of the electrospun fibre mats and the dispersion of the cut electrospun fibres, the PTMC concentration was maintained below 40 wt%, above which the viscosity was found to be too high for effective impregnation and processing. Too low concentrations, on the other hand, result in delayed curing, low crosslink densities and poor mechanical properties. The rheological profile of PTMC resin during curing is presented in Fig. 5. In these experiments, UV exposure was started at 20 sec and lasted for 90 sec. For all three concentrations, loss modulus G" was initially higher than storage modulus G', indicating a viscous fluid behaviour. With increasing UV exposure time, both G' and G" increased and crossed over at the gelation point. It was observed that the time to sol-gel transition for the 20 wt% resin was longer than for 30 wt% and 40 wt% resins.

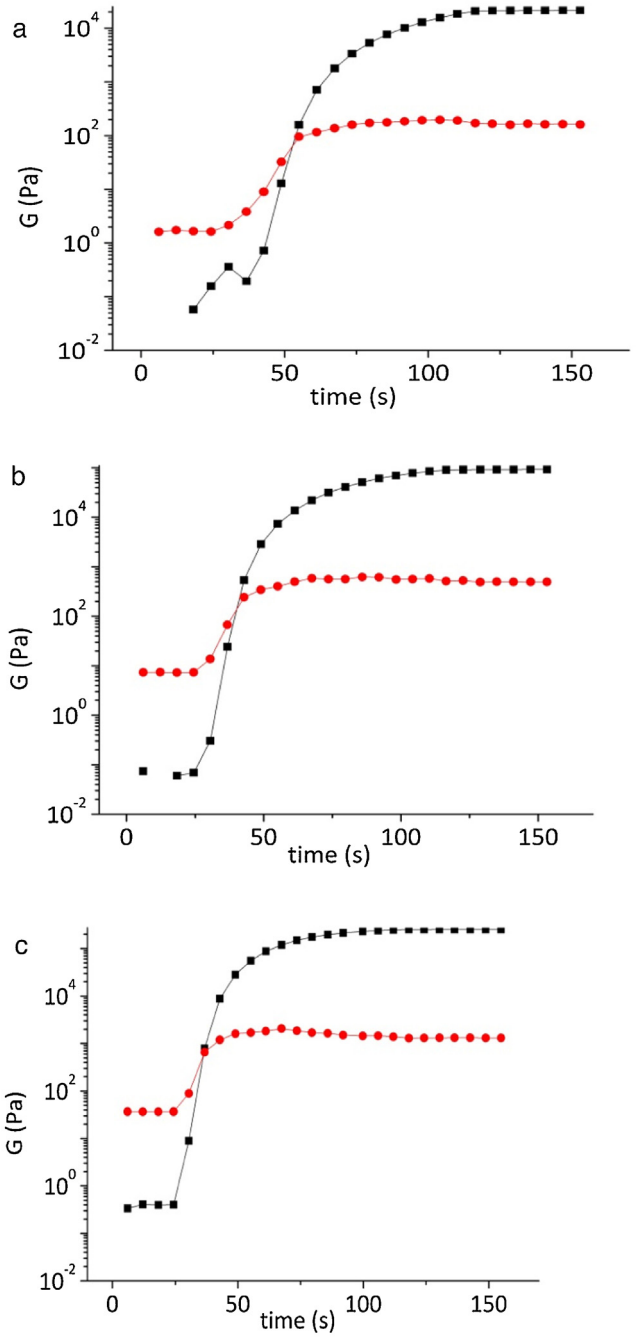

Fig. 5. Rheological profiles of PTMC/propylene carbonate solution cured under UV, as a function of time: a. 20 wt% PTMC, b. 30 wt% PTMC and c. 40 wt% PTMC (UV started at 20 sec for 90 sec at an intensity of 15 mW/cm^2, frequency 1 Hz, strain 0.1%). Black squares, shear storage modulus; red circles, shear loss modulus. (For interpretation of the references to colour in this figure legend, the reader is referred to the web version of this article.).

This is attributed to the lower density of crosslinking groups and potentially stronger impact of oxygen concentration at lower concentrations. Afterwards G' overtook G" and continued increasing although at a slower rate. It reached a plateau near 90 sec of exposure and stopped progressing further as photoinitiation was not maintained. Thus, the optimal UV exposure time for preparing the PTMC resin and its composites was set at 90 sec in all further experiments. In addition, resins formed from 40 wt% solutions displayed a higher G' and a lower degree of shrinkage than those prepared from 30 wt% solutions. Therefore, the optimal concentration of PTMC in

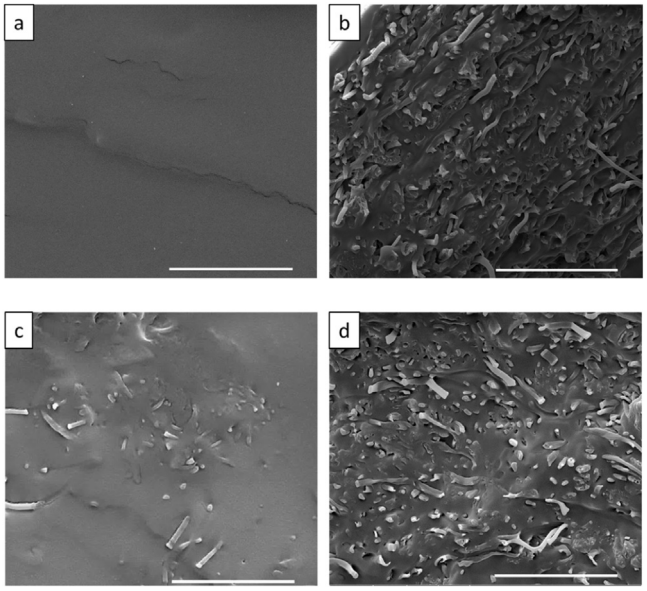

Fig. 6. SEM images of the cold fractured surface of PTMC-fibre composites: a. neat PTMC; b. continuous fibre composite; c. 5 wt% short fibre composite; d. 30 wt% short fibre composite (scale bar: 20 μm).

solutions used to impregnate fibres and prepare composites was set at 40 wt%.

Neat PTMC and PTMC/PLA fibre composite samples were produced using 40 wt% macromer solutions. SEM images of these composites are presented in Fig. 6. During processing, it was noticed that the matrix solution readily impregnated the PLA fibre mats, implying excellent wetting ability, presumably favoured by the high porosity of the fibre network [28,40]. However, considering the low volatility of propylene carbonate, this solvent has to be removed after UV curing through extraction using a diluted propylene carbonate/ethanol solution. By reducing the propylene carbonate/ethanol ratio, propylene carbonate trapped in the crosslinked PTMC slowly diffused out. The removal of propylene carbonate resulted in shrinkage of PTMC by 69.8 ± 5.6 vol%. Gradual reduction in propylene carbonate content was important to control the stress accumulation during extraction, especially for the PTMC-fibre composites and avoid loss of the sample's integrity. After extraction, the PTMC-rich areas that were not fully incorporated into the fibre mat (on the side of samples) were removed. This protocol resulted in composite films with a thickness of around 110 μm (measured for each sample). By comparing the mass of the electrospun fibre mat incorporated and that measured for the PTMC/long fibre composites, the weight percentage of fibres in the composite was calculated as varied from 16.5 wt% to 22.9 wt% with average value of 20.0 ± 1.7 wt%. In the case of continuous electrospun fibre mats, the interconnected pores were completely filled with PTMC resin and no obvious voids were present in SEM, which supports the good wetting and impregnation of PTMC resin into the PLA fibre mats. Only a thin layer of PTMC was observed at the composite surface; this layer was formed during the fabrication process and did not contain any fibres. The roughness of the PTMC fracture surface was increased with the incorporation of PLA fibres. All fracture surfaces indicated good levels of adhesion and interaction between the electrospun PLA fibres and the PTMC matrix with little evidence of fibre pull-out. This is indicative of good stress transfer between PLA fibres and PTCM matrix and a high reinforcing ability of the electrospun fibres.

PTMC/short fibre composites were also characterized using SEM. By increasing the content of short fibres, the fracture surfaces of the PTMC composites became rougher. Again very few

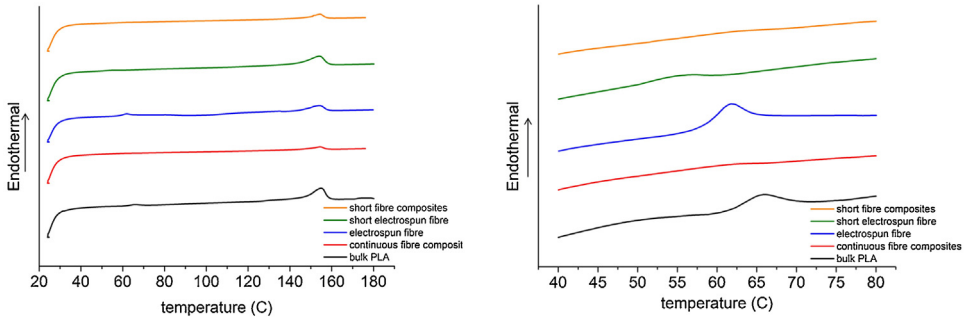

Fig. 7. Thermal properties of bulk PLA (black), continuous electrospun PLA fibres (blue), short electrospun PLA fibres (green), continuous fibre composite (red), 30 wt% short fibre composite (orange). (For interpretation of the references to colour in this figure legend, the reader is referred to the web version of this article.)

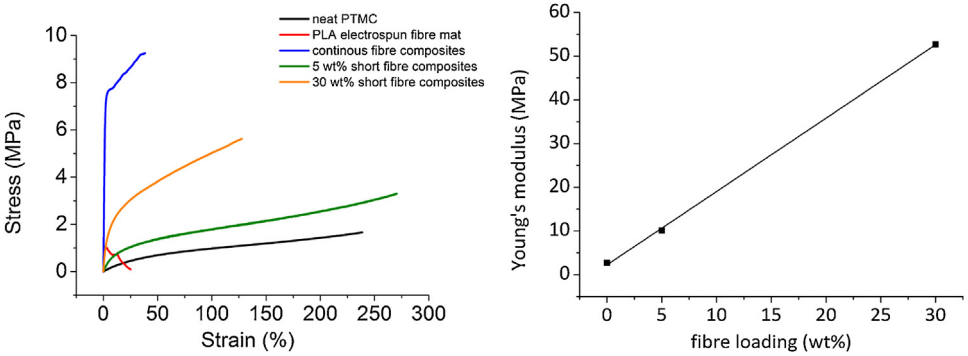

Fig. 8. (left) Stress-strain curve of neat PTMC and PTMC/PLA fibre composites: neat PTMC (black), neat electrospun PLA fibre mats (red), continuous fibre mat composites (blue), 5 wt% short fibres composites (green), 30 wt% short fibre composite (orange). (right) Dependence of composite Young's modulus on short fibre loading. (For interpretation of the references to colour in this figure legend, the reader is referred to the web version of this article.)

voids or fibre pull-outs could be observed after fracture, indicating a good dispersion and interaction of the PLA fibres with the polymer matrix. Compared to composites based on electrospun mats, short fibres provide more processing flexibility. The amount of fibres in the composite can be easily tuned by adding more or less fibres in the resin, while for mat-based composites, the amount of fibres is limited by the porosity of the mat. Simply casting more resin onto the electrospun fibre mats may to some extent alter the PTMC/fibre ratio but will ultimately result in resin rich layers of pure PTMC on the surface of the composite. More importantly, short fibre reinforced PTMC composites can be easily moulded into complex shapes via injection or compression moulding or 3D printing while continuous fibre composites can only be made into simple double curved shapes due to the fibre mat structure. Issues with short fibres composites and particularly nanofibre composites are related to an uneven distribution of fibres in the matrix as a result of aggregation. Some fibres were found to aggregate while also some resin rich areas were observed. The fibre aggregation is due to the interaction between the nanofibres. The average length of the short electrospun fibres is 220 μm while some were as long as 700 μm. Similar to other high aspect ratio nanoparticles such as carbon nanotubes, the high aspect ratio of these fibres (which can be as high as 300) will inevitably induce some fibre entanglement or network formation due to fibre–fibre interaction [41,42].

3.3. Thermo-mechanical properties of PTMC and PTMC/fibre composites

Thermal properties of PLA electrospun fibre and PTMC/fibre composites were characterized by DSC and presented in Fig. 7. T_g of PTMC is measured at −13.5° C (graph not shown) and was not affected by the incorporation of PLA fibres, consistent with low interpenetration of the two networks. A second polyester-associated T_g was observed for as-spun PLA fibres and fibres in PTMC composites, near 60° C, which is lower than the T_g of bulk PLA (63.9° C). The decrease of T_g can be explained by polymer chain orientation during electrospinning, which drives molecules to become mobile at lower temperature [43]. T_g of short electrospun PLA fibres is 53° C, presumably due to small traces of residual solvents from cutting process. All samples showed melting points near 154° C. In addition, as-spun PLA fibres showed cold crystallization, which is not observed on other samples. The crystallinity of bulk PLA, as-spun PLA fibres, short PLA fibres, continuous PLA fibres in composites and short PLA fibres in composites are 34.4%, 3.4%, 35.1%, 55.6% 32.8% respectively. The increase of PLA crystallinity after processing into short- and/or continuous fibre composites is due to the solvent treatment effect [44]. The crystallinity of short fibres was found to be lower than that measured for continuous fibre in composites, possibly as a result of lower PLA chain orientation.

The stress-strain profiles recorded for pure PTMC, electrospun fibre mat and composites are shown in Fig. 8. Quantification of mechanical data is listed in Table 1. PLA electrospun fibre mats have poor mechanical properties due to random fibre orientation, fibre bending and fibre–fibre sliding when stretching. Compared with neat PTMC, the Young's modulus of the PTMC composites reinforced with continuous PLA fibre mats (20 wt%) is improved by more than two orders of magnitude. Tensile strength was increased 5-fold and toughness was doubled. The increase in Young's modulus, tensile strength and toughness implies an efficient reinforcement of the mechanical properties of PTMC by PLA electrospun fibres. As expected, the elongation at break of PTMC is decreased after incorporating long electrospun PLA fibres. The low failure strain of these composites can be attributed to the low failure strain of PLA fibres. According to the results of tensile test, electrospun PLA fibre mats exhibited a low failure strain (near 20%), which is however higher than the failure strain of bulk PLA (near

Table 1
Summary of tensile test results of PTMC, electrospun PLA fibre mat and PTMC/PLA fibre composites.

Sample	Young's modulus (MPa)[a]	Tensile strength (MPa)	Elongation at break (%)	Toughness (MPa)
PTMC	2.7 ± 0.1	1.3 ± 0.1	199 ± 31	1.6 ± 0.4
PLA electrospun fibre mat	46.2 ± 8.8	1.2 ± 0.4	19.9 ± 7.9	0.2 ± 0.1
Continuous fibre mat composite	310 ± 87	7.5 ± 1.7	46.2 ± 4.1	3.3 ± 0.7
5 wt% short fibre composite	10.1 ± 0.3	3.4 ± 0.1	289 ± 30	5.9 ± 0.7
30 wt% short fibre composite	52.7 ± 8.7	5.9 ± 0.7	141 ± 19	6.1 ± 1.5

[a] Young's moduli were calculated by the slope of the stress-strain curve at 2% strain.

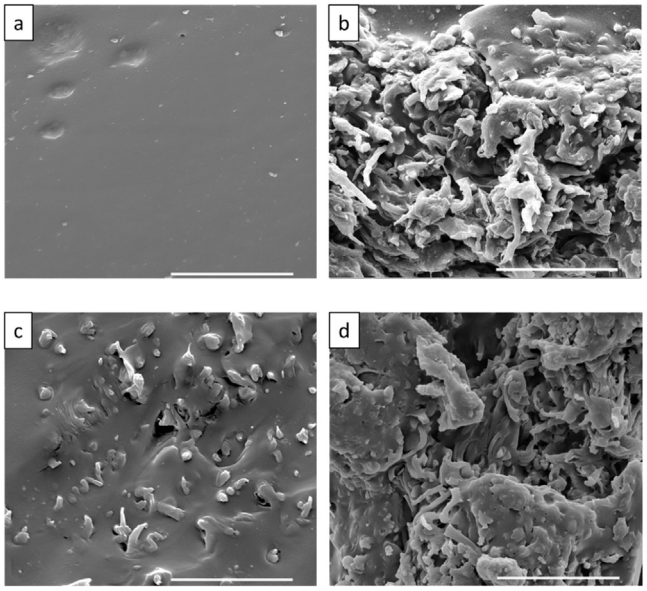

Fig. 9. SEM images of the fracture surface of neat PTMC and PTMC/PLA fibre composites after tensile testing: a. neat PTMC; b. continuous fibre composite; c. 5 wt% short fibre composite; d. 30 wt% short fibre composite (scale bar: 20 μm).

9%) [45], due to the deformation mechanisms in these non-wovens. The SEM images of tensile fracture surfaces are shown in Fig. 9. Neat PTMC samples exhibit a smooth fracture surface while long fibre reinforced PTMC has a rough one. Some fibre protrusions can be seen at the surface but most fibres were strongly embedded in the matrix (Fig. 9b). This again suggests a strong bonding between the PLA fibre and PTMC matrix.

PTMC composites based on short electrospun PLA fibres also showed an improvement in mechanical properties. With addition of merely 5 wt% short fibres, the E-modulus, tensile strength and toughness were increased 3 times compared with neat PTMC. Interestingly, in the case of short fibre composites the elongation of break was not affected by the addition of PLA fibres. Moreover, unlike long fibre composites, composites with 5 wt% short PLA fibres did not show the marked non-linear behaviour at low strain. Instead it maintained a good ductility similar to neat PTMC. The improvement in Young's modulus and strength is again an indicator of the effective reinforcement of the PTMC by PLA fibres. Compared with self-reinforced PI/PI short fibre composites [20], at similar fibre loading level, reinforcement in the PTMC/PLA short fibre composites was found to be more significant due to the greater property mismatch between PLA fibres and PTMC matrix. As the short fibre loading increases, the composite's Young's modulus increased linearly (see Fig. 8). At 30 wt% PLA fibres, the modulus increased by 20 times. Tensile strength increased by 4.5 times but at a much slower rate than the Young's modulus. Interestingly, the toughness of these composites is similar to those of low fibre loadings. The elongation at break was however decreased significantly in comparison with short fibre composites incorporating 5 wt% PLA fibres. There is little evidence of fibre pull-out in the short fibre composites; instead, a failure mode involving fibre breakage was observed, suggesting that the PLA fibre length is beyond the critical length [46]. The fibre critical length (L_c) is defined by $L_c = \sigma_f D/2\tau$, where σ_f is the fibre strength, D is fibre diameter and τ is the interfacial strength [47]. When perfect adhesion between fibre and matrix is assumed, the interfacial strength (τ) can be estimated from the tensile strength of matrix (1.3 MPa by tensile test) using Von Mises yield criterion ($1.3/\sqrt{3}$ MPa) [48]. Fibre strength of 53 MPa (data provided by supplier) and diameter (600 nm) were used together with τ ($1.3/\sqrt{3}$ MPa) to estimate L_c. The L_c is calculated as 21 μm, which is one magnitude less than the average length of short fibre (220 μm), indicating high reinforcement efficiency of short fibres.

A modified rule of mixture (MROM) was used to evaluate the experimental data of the electrospun fibre-reinforced composites [46,49]. In such analysis, perfect interfacial adhesion between fibres and matrix as well as a homogeneous distribution of fibres in the matrix were assumed. The MROM equation predicting the Young's modulus of a composite is:

$$E_c = \chi_1 \chi_2 V_f E_f + V_m E_m \quad (1)$$

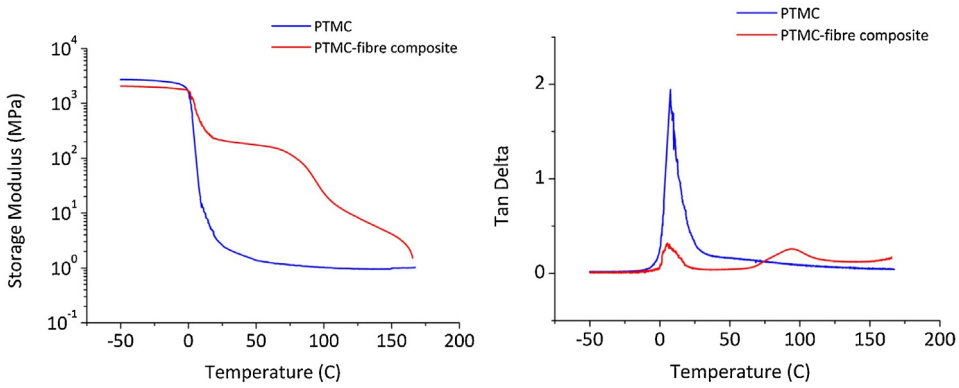

Fig. 10. DMA results of neat PTMC and PTMC/continuous fibre composites: (left) storage modulus as a function of temperature; (right) Tan Delta as a function of temperature (blue-neat PTMC, red-PTMC/fibre composites). (For interpretation of the references to colour in this figure legend, the reader is referred to the web version of this article).

Table 2
Comparison of theoretical predictions using MROM with experimental data.

Sample	Fibre volume fraction V_f (%)	Matrix volume fraction V_m (%)	E_f (MPa) × 10-3	E_m (MPa)	Fibre orientation factor $\chi 1$	Fibre length factor $\chi 2$	E_c[a] (MPa)	E_{cE}[b] (MPa)
5 wt% short fibre composite	4.8	95.2	3.5	2.7	1/5	0.86	31.5	10.1
30 wt% short fibre composite	23.3	76.7	3.5	2.7	1/5	0.90	149	53

[a] E_c is the short fibre composite modulus derived from the MROM.
[b] E_{cE} is the composite modulus obtained from the experimental tensile tests.

In this equation, χ_1 and χ_2 represent the fibre orientation and length efficiency factors, respectively. E_c, E_f and E_m are the Young's modulus of the composite, PLA fibres and matrix material (PTMC), respectively. The volume fractions V_f and V_m are derived from the weight ratio of PLA fibres to PTMC matrix. A density of 1.247 g/cm^3 was measured for PTMC, using a density meter. The density of PLA was taken as 1.24 g/cm^3, based on the product data provided by the supplier for bulk PLA. Hence, for continuous fibre mat composites (20 wt%), the volume fractions of fibre and matrix are calculated as 20.1% and 79.9% respectively. The length efficiency factor χ_2 for continuous fibre mat composites is 1 and can be ignored. The orientation factor χ_1 is defined as 3/8 for in-plane (2D) randomly distributed fibres [50,51]. Thus Eq. (1) can be transformed into;

$$E_c = \frac{3}{8} V_f E_f + V_m E_m \tag{2}$$

In this equation, E_m (2.7 MPa) was directly obtained from tensile test of PTMC. E_c of continuous fibre mat composite (310 MPa by tensile test) was used in Eq. (2) and PLA fibre modulus E_f of 4.1 GPa was back-calculated, which is slightly higher than that of bulk PLA (3.5 GPa as provided by supplier). This is because electrospinning will, to some extent, align the polymer chains within fibres. It was reported thin electrospun fibres (usually 200–300 nm in diameter) had a three-fold increase in Young's modulus compared to that of bulk polymer however thicker fibres (>300 nm in diameter) will only have insignificant increase [52]. The Young's modulus of single PLA electrospun fibres with diameter of 350 nm can even reach as high as 8 GPa by earlier report [26]. In our case, fibres have an average diameter of 600 nm, which is expected to have limited increase in E_f. And it is supported by the back-calculated Young's modulus of fibre (4.1 GPa) compared to that of bulk PLA (3.5 GPa).

For short fibre composites, the length factor χ_2 has to be considered. Here, the orientation factor χ_1 is defined as 1/5 because the fibres are considered to be randomly (3D) distributed throughout the matrix [50,51]. The length efficiency factor χ_2 can be estimated using Eq. (3) [53];

$$\chi_2 = 1 - \frac{\tanh(a \cdot \frac{L}{d})}{a \cdot \frac{L}{d}} \tag{3}$$

with

$$a = \sqrt{\frac{-3}{2 \ln V_f} \cdot \frac{E_m}{E_f}} \tag{4}$$

In this equation, L is the mean length of the discontinuous fibres; d is the average fibre diameter; a is a coefficient. The value of χ_2 is then calculated and the composite modulus E_c can be predicted using Eq. (1), in which E_m (2.7 MPa) was obtained from tensile test and E_f (3.5 GPa) was provided by the bulk PLA supplier. The results are listed in Table 2.

In our composites, the mean fibre length is around 220 μm compared to a critical length of 21 μm for the PTCM/PLA fibre system. The calculated fibre length efficiency factors χ_2 are therefore close to $\chi_2 = 1$ (0.86 and 0.90, respectively) as fibre length is well above the critical length ($L > 10\,L_c$) [46]. For short electrospun fibre-reinforced composites, the theoretical predictions overestimate the experimental data. This can be explained by some of the fibre aggregation in these systems as observed by SEM. The MROM assumes a homogeneous distribution of fibres in matrix. Fibres should be uniformly and randomly dispersed throughout the matrix and each fibre be fully covered by matrix [54]. In the case of fibre aggregation, the fibre orientation factor χ_1 is affected. The interfacial contact area between fibres and matrix is inhibited and therefore the stress transfer between fibres and matrix becomes less efficient. Moreover, aggregation also changes the fibre aspect ratio. Thus the fibre length efficiency factor χ_2 is decreased [55]. Meanwhile, aggregation of fibres will also introduce stress concentrations, which will be accompanied by a decrease in composite strength. Another issue to consider is the effect of the fibre cutting procedure on fibre properties, such as decrease in crystallinity. All of these effects may lead to an overestimation in composite properties, but overall by a reasonably small factor (calculations predict moduli three-fold higher than the experimental values).

3.4. Temperature dependence of mechanical properties of PTMC/fibre composites

DMA was performed on both neat PTMC and its continuous fibre mat composites. The evolution of the storage modulus (G') and tan (δ) as a function of temperature is presented in Fig. 10. Experiments began at −50° C and ended at 170 ° C. At low temperatures, well below the PTMC glass transition temperature (T_g), the storage modulus of both samples was initially very high (2.3–2.7 GPa). With increasing temperatures, the modulus decreased slowly until a rapid drop occurred at 7.5 ° C. Meanwhile the Tan Delta of both samples also reached its peak value, corresponding to the glass transition temperature of the PTMC matrix. With increasing temperatures, a second drop in storage modulus is observed for the PTMC/PLA fibre composite. A second peak also appeared in the Tan Delta curve of the composite, indicating the glass transition of the electrospun PLA fibres. Upon further heating the storage modulus of the composite continues to decrease until reaching the PLA melting point while the crosslinked PTMC matrix maintains a rubber plateau modulus of around 1 MPa. Furthermore, the storage modulus for crosslinked PTMC and PTMC/nanofibre composite at body temperature (37° C) are 1.8 MPa and 190 MPa respectively. Hence, these results indicate the significant benefit of loading electrospun PLA fibres within PTMC matrices, in terms of material stiffness, improving the mechanical properties and dimensional stability of PTMC in conditions typically experienced for tissue engineering applications.

4. Conclusions

Electrospun PLA fibre reinforced PTMC composites were successfully prepared and characterized. A new method of cutting electrospun PLA fibres with lengths ranging from 50 to 700 μm using solvent-assisted mechanical stirring was reported. These short fibres were then incorporated into PTMC matrix to produce short nanofibre reinforced composites. Their mechanical properties were tested and compared with those based on electrospun

PLA fibre mats, and were analysed using a simple micromechanical model. The mechanical properties of PTMC were improved for both continuous and short fibres. PTMC is found to be significantly enhanced by the incorporation of fibre mats (more than 100 times in Young's modulus). It is stiffer and stronger than short fibre enhanced composites due to fibre continuity and high aspect ratio. However, the ductility and toughness of these composites are significantly decreased compared to short fibre composites. Composites based on short fibres also exhibited a high reinforcing efficiency. Even with the addition of a small amount (5 wt%) of short PLA fibres, the Young's modulus and tensile strength improved significantly without compromising the ductility of PTMC.

Besides interesting mechanical characteristics, the developed short fibre composites are of particular interest due to their potential processing advantage over traditional electrospun fibre reinforced composites based on fibre mats. Short fibre composites can be processed via liquid formulations moulding (injection and compression) or into complex shapes via 3D plotters or stereolithography.

The developed electrospun PLA fibre reinforced PTMC composites, being based on materials already well-established for biomedical applications, are expected to be nontoxic and biodegradable. Their improved mechanical performance and dimensional stability makes them interesting candidates for many tissue engineering applications. For example, short PLA fibres can be incorporated in PTMC resin and used to create complex scaffolds by stereolithography or 3D printing. Moreover, the electrospun PLA fibres could be loaded with a drug which when embedded in a PTMC matrix can lead to novel drug release systems.

Acknowledgements

The authors acknowledge the funding provided by NSFC-DG-RTD Joint Scheme (Project No. 51361130034) and the RAPIDOS project under the European Union's 7th Framework Programme (Project No.604517).

References

[1] W.H. Carothers, G.L. Dorough, F.J. van Natta, Studies of polymerization and ring formation: x. The reversible polymerization of six-membered cyclic esters, J. Am. Chem. Soc. 54 (1932) 761–772.
[2] K. Fukushima, Poly(trimethylene carbonate)-based polymers engineered for biodegradable functional biomaterials, Biomater. Sci. 4 (2015) 9–24.
[3] H. Li, J. Chang, Y. Qin, Y. Wu, M. Yuan, Y. Zhang, Poly(lactide-co-trimethylene carbonate) and polylactide/polytrimethylene carbonate blown films, Int. J. Mol. Sci. 15 (2014) 2608–2621.
[4] J. Han, C.J. Branford-White, L.-M. Zhu, Preparation of poly(ε-caprolactone)/poly(trimethylene carbonate) blend nanofibers by electrospinning, Carbohydr. Polym. 79 (2010) 214–218.
[5] J. Kim, J. Lee, Preparation and properties of poly(L-lactide)-block-poly(trimethylene carbonate) as biodegradable thermoplastic elastomer, Polym. J. 34 (2002) 203–208.
[6] A.P. Pêgo, D.W. Grijpma, J. Feijen, Enhanced mechanical properties of 1,3-trimethylene carbonate polymers and networks, Polymer 44 (2003) 6495–6504.
[7] L.-Q. Yang, B. He, S. Meng, J.-Z. Zhang, M. Li, J. Guo, et al., Biodegradable cross-linked poly(trimethylene carbonate) networks for implant applications: synthesis and properties, Polymer 54 (2013) 2668–2675.
[8] E. Bat, T.G. van Kooten, J. Feijen, D.W. Grijpma, Resorbable elastomeric networks prepared by photocrosslinking of high-molecular-weight poly(trimethylene carbonate) with photoinitiators and poly(trimethylene carbonate) macromers as crosslinking aids, Acta Biomater. 7 (2011) 1939–1948.
[9] S. Schuller-Ravoo, J. Feijen, D.W. Grijpma, Flexible, elastic and tear-resistant networks prepared by photo-crosslinking poly(trimethylene carbonate) macromers, Acta Biomater. 8 (2012) 3576–3585.
[10] A.C. van Leeuwen, R.R. Bos, D.W. Grijpma, Composite materials based on poly(trimethylene carbonate) and beta-tricalcium phosphate for orbital floor and wall reconstruction, J. Biomed. Mater. Res. Part B: Appl. Biomater. 100 (2012) 1610–1620.
[11] S. Lin, Q. Cai, J. Ji, G. Sui, Y. Yu, X. Yang, et al., Electrospun nanofiber reinforced and toughened composites through in situ nano-interface formation, Compos. Sci. Technol. 68 (2008) 3322–3329.
[12] A. Greiner, J.H. Wendorff, Electrospinning: a fascinating method for the preparation of ultrathin fibers, Angew. Chem. 46 (2007) 5670–5703.
[13] J. Yao, C. Bastiaansen, T. Peijs, High strength and high modulus electrospun nanofibers, Fibers 2 (2014) 158–186.
[14] M.M. Bergshoef, G.J. Vansco, Transparent nanocomposites with ultrathin, electrospun nylon-4, 6 fiber reinforcement, Adv. Mater. 11 (1999) 1362–1365.
[15] Y. Dong, T. Mosaval, H.J. Haroosh, R. Umer, H. Takagi, K.-T. Lau, The potential use of electrospun polylactic acid nanofibers as alternative reinforcements in an epoxy composite system, J. Polym. Sci. B: Polym. Phys. 52 (2014) 618–623.
[16] U. Stachewicz, F. Modaresifar, R.J. Bailey, T. Peijs, A.H. Barber, Manufacture of void-free electrospun polymer nanofiber composites with optimized mechanical properties, ACS Appl. Mater. Interfaces 4 (2012) 2577–2582.
[17] J. Yao, G. Li, C.W.M. Bastiaansen, T. Peijs, High performance co-polyimide nanofiber reinforced composites, Polymer 76 (2015) 46–51.
[18] Y. Zuo, F. Yang, J.G. Wolke, Y. Li, J.A. Jansen, Incorporation of biodegradable electrospun fibers into calcium phosphate cement for bone regeneration, Acta Biomater. 6 (2010) 1238–1247.
[19] Z.-M. Huang, Y.Z. Zhang, M. Kotaki, S. Ramakrishna, A review on polymer nanofibers by electrospinning and their applications in nanocomposites, Compos. Sci. Technol. 63 (2003) 2223–2253.
[20] S. Jiang, G. Duan, J. Schöbel, S. Agarwal, A. Greiner, Short electrospun polymeric nanofibers reinforced polyimide nanocomposites, Compos. Sci. Technol. 88 (2013) 57–61.
[21] S.-Y. Fu, Y.-W. Mai, B. Lauke, C.-Y. Yue, Synergistic effect on the fracture toughness of hybrid short glass fiber and short carbon fiber reinforced polypropylene composites, Mater. Sci. Eng. A 323 (2002) 326–335.
[22] N.G. Karsli, A. Aytac, V. Deniz, Effects of initial fiber length and fiber length distribution on the properties of carbon-fiber-reinforced-polypropylene composites, J. Reinf. Plast. Compos. 31 (2012) 1053–1060.
[23] H.S. Yoo, T.G. Kim, T.G. Park, Surface-functionalized electrospun nanofibers for tissue engineering and drug delivery, Adv. Drug Deliv. Rev. 61 (2009) 1033–1042.
[24] M. Jamshidian, E.A. Tehrany, M. Imran, M. Jacquot, S. Desobry, Poly-lactic acid: production, applications, nanocomposites, and release studies, Compr. Rev. Food Sci. Food Saf. 9 (2010) 552–571.
[25] J.R. Sarasua, Arraiza A. Lp, P. Balerdi, I. Maiza, Crystallinity and mechanical properties of optically pure polylactides and their blends, Polym. Eng. Sci. 45 (2005) 745–753.
[26] X. Zhang, R. Nakagawa, K.H.K. Chan, M. Kotaki, Mechanical property enhancement of polylactide nanofibers through optimization of molecular weight, electrospinning conditions, and stereocomplexation, Macromolecules 45 (2012) 5494–5500.
[27] F. Mai, W. Tu, E. Bilotti, T. Peijs, The influence of solid-state drawing on mechanical properties and hydrolytic degradation of melt-spun Poly(Lactic acid) (PLA) tapes, Fibers 3 (2015) 523–538.
[28] K. Odelius, A. Hoglund, S. Kumar, M. Hakkarainen, A.K. Ghosh, N. Bhatnagar, et al., Porosity and pore size regulate the degradation product profile of polylactide, Biomacromolecules 12 (2011) 1250–1258.
[29] S. Schuller-Ravoo, S.M. Teixeira, J. Feijen, D.W. Grijpma, A.A. Poot, Flexible and elastic scaffolds for cartilage tissue engineering prepared by stereolithography using poly(trimethylene carbonate)-based resins, Macromol. Biosci. 13 (2013) 1711–1719.
[30] M.A. Geven, V. Varjas, L. Kamer, X. Wang, J. Peng, D. Eglin, et al., Fabrication of patient specific composite orbital floor implants by stereolithography, Polym. Adv. Technol. 26 (2015) 1433–1438.
[31] A.P. Mathew, K. Oksman, M. Sain, The effect of morphology and chemical characteristics of cellulose reinforcements on the crystallinity of polylactic acid, J. Appl. Polym. Sci. 101 (2006) 300–310.
[32] E. Mulky, G. Yazgan, K. Maniura-Weber, R. Luginbuehl, G. Fortunato, Buhlmann-popa AM fabrication of biopolymer-based staple electrospun fibres for nanocomposite applications by particle-assisted low temperature ultrasonication, Mater. Sci. Eng. C Mater. Biol. Appl. 45 (2014) 277–286.
[33] M. Sawawi, T.Y. Wang, D.R. Nisbet, G.P. Simon, Scission of electrospun polymer fibres by ultrasonication, Polymer 54 (2013) 4237–4252.
[34] A. Stoiljkovic, S. Agarwal, Short electrospun fibers by UV cutting method, Macromol. Mater. Eng. 293 (2008) 895–899.
[35] O. Kriha, M. Becker, M. Lehmann, D. Kriha, J. Krieglstein, M. Yosef, et al., Connection of hippocampal neurons by magnetically controlled movement of short electrospun polymer fibers—a route to magnetic micromanipulators, Adv. Mater. 19 (2007) 2483–2485.
[36] I.W. Fathona, A. Yabuki, A simple one-step fabrication of short polymer nanofibers via electrospinning, J. Mater. Sci. 49 (2014) 3519–3528.
[37] I.W. Fathona, A. Yabuki, Short electrospun composite nanofibers: effects of nanoparticle concentration and surface charge on fiber length, Curr. Appl. Phys. 14 (2014) 761–767.
[38] I.W. Fathona, A. Yabuki, One-step fabrication of short electrospun fibers using an electric spark, J. Mater. Process. Technol. 213 (2013) 1894–1899.
[39] F. Inam, M.J. Reece, T. Peijs, Shortened carbon nanotubes and their influence on the electrical properties of polymer nanocomposites, J. Compos. Mater. 46 (2011) 1313–1322.
[40] X. Zhu, W. Cui, X. Li, Y. Jin, Electrospun fibrous mats with high porosity as potential scaffolds for skin tissue engineering, Biomacromolecules 9 (2008) 1795–2008.
[41] F. Inam, D.W.Y. Wong, M. Kuwata, T. Peijs, Multiscale hybrid micro-nanocomposites based on carbon nanotubes and carbon fibers, J. Nanomater. 2010 (2010) 1–12.

[42] D. Wu, L. Wu, W. Zhou, Y. Sun, M. Zhang, Relations between the aspect ratio of carbon nanotubes and the formation of percolation networks in biodegradable polylactide/carbon nanotube composites, J. Polym. Sci. B: Polym. Phys. 48 (2010) 479–489.
[43] W. Cui, X. Li, X. Zhu, G. Yu, S. Zhou, J. Weng, Investigation of drug release and matrix degradation of electrospun poly (DL-lactide) fibers with paracetanol inoculation, Biomacromolecules 7 (2006) 1623–1629.
[44] S. Sato, D. Gondo, T. Wada, S. Kanehashi, K. Nagai, Effects of various liquid organic solvents on solvent-induced crystallization of amorphous poly(lactic acid) film, J. Appl. Polym. Sci. 129 (2012) 1607–1617.
[45] O. Martin, L. Avérous, Poly(lactic acid): plasticization and properties of biodegradable multiphase systems, Polymer 42 (2001) 6209–6219.
[46] S.-Y. Fu, B. Lauke, Effects of fiber length and fiber orientation distributions on the tensile strength of short-fiber-reinforced polymers, Compos. Sci. Technol. 56 (1996) 1179–1190.
[47] J.L. Thomason, M.A. Vlug, G. Schipper, Krikor H.G.L.T, Influence of fibre length and concentration on the properties of glass fibre-reinforced polypropylene: part 3 Strength and strain at failure, Compos. Part A: Appl. Sci. Manuf. 27 (1996) 1075–1084.
[48] T. Peijs, S. Garkhail, R. Heijenrath, M. van Den Oever, H. Bos, Thermoplastic composites based on flax fibres and polypropylene: influence of fibre length and fibre volume fraction on mechanical properties, Macromol. Symp. 127 (1998) 193–203.
[49] Z. Yu, J. Brisson, A. Ait-Kadi, Prediction of mechanical properties of short Kevlar fiber-nylon-6, 6 composites, Polym. Compos. 15 (1994) 64–73.
[50] S. Garkhail, R. Heijenrath, T. Peijs, Mechanical properties of natural-fibre-mat-reinforced thermoplastics based on flax fibres and polypropylene, Appl. Compos. Mater. 7 (2000) 351–372.
[51] H. Krenchel, Fibre Reinforcement, Akademisk Forlag, Copenhagen, Denmark, 1964.
[52] M. Naraghi, S.N. Arshad, I. Chasiotis, Molecular orientation and mechanical property size effects in electrospun polyacrylonitrile nanofibers, Polymer 52 (2011) 1612–1618.
[53] G.P. Carman, K.L. Reifsnider, Micromechanics of short-fiber composites, Compos. Sci. Technol. 43 (1992) 137–146.
[54] J.N. Coleman, U. Khan, W.J. Blau, Y.K. Gun'ko, Small but strong: a review of the mechanical properties of carbon nanotube—polymer composites, Carbon 44 (2006) 1624–1652.
[55] M.A.L. Manchado, L. Valentini, J. Biagiotti, J.M. Kenny, Thermal and mechanical properties of single-walled carbon nanotubes–polypropylene composites prepared by melt processing, Carbon 43 (2005) 1499–1505.